JOC The Journal of Organic Chemistry Cite This: J. Org. Chem. XXXX, XXX, XXX−XXX Article pubs.acs.org/joc

Pyrrolo[2,3-*d*:5,4-*d*′]bisthiazoles: Alternate Synthetic Routes and a Comparative Study to Analogous Fused-Ring Bithiophenes

Eric J. Uzelac, Casey B. McCausland, and Seth C. Rasmussen*

Department of Chemistry and Biochemistry, North Dakota State University, NDSU Dept. 2735, P.O. Box 6050, Fargo, North Dakota 58108-6050, United States

Supporting Information

ABSTRACT: New synthetic methods have been developed for the preparation of 4-alkyl- and 4-aryl-pyrrolo[2,3-*d*:5,4-*d*′]bisthiazole (PBTz) building blocks from 2,4-thiazolidinedione. The resulting PBTz products have been fully characterized via structural, electronic, and optical methods, thus allowing full comparison to the previously reported dithieno[3,2-*b*:2′,3′-*d*]pyrrole (DTP) analogues. Such comparisons then allow a detailed discussion of the relative electronic effects of the various methods utilized to tune the properties of the parent DTP building block.

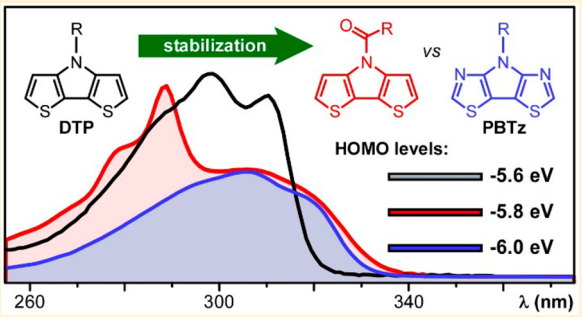

INTRODUCTION

Conjugated organic materials continue to receive considerable fundamental and technological interest, with particular focus on their development for applications such as sensors, electrochromic devices, field-effect transistors (FETs), organic photovoltaics (OPVs), and organic light-emitting diodes (OLEDs).[1−3] One of the many strengths of these materials has been the ability to tune their desirable electronic and optical properties at the molecular level via synthetic modification. In this respect, thiophene-based materials have been found to be especially popular due to their ease of synthetic manipulation.[2,3] One popular approach to modulating thiophene-based materials through structural modification has been the application of fused-ring units, particularly fused 2,2′-bithiophenes such as cyclopenta[2,1-*b*:3,4-*b*′]dithiophene (CDT),[2−6] silolo[3,2-*b*:4,5-*b*′]dithiophene (SDT),[3−5] dithieno[3,2-*b*:2′,3′-*d*]pyrrole (DTP),[2−9] and phospholo[3,2-*b*:4,5-*b*′]dithiophene (PDT),[3−5] germolo[3,2-*b*:4,5-*b*′]-dithiophene (GDT),[3,10−12] and arsolo[3,2-*b*:4,5-*b*′]-dithiophene (ADT)[13−15] as shown in Chart 1. The fused-ring nature of these species enhances the planar nature of the ground state, leading to improved conjugation, increased delocalization, and lower band gaps, while also reducing contributions of interannular torsional vibrations, potentially leading to increased emission quantum yields. In addition, the bridging unit (ER or ER_2) can modulate the electronics via inductive effects to tune the corresponding HOMO or LUMO energies, while the central placement of the side chains allows the use of fairly bulky groups with limited steric interactions that can lead to reduced backbone planarity in the resulting materials.[5,6]

Chart 1. Fused 2,2′-Bithiophene Building Blocks

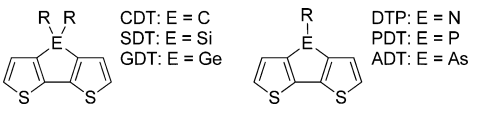

Of the bridged 2,2′-bithiophenes given in Chart 1, the nitrogen-bridged DTP building blocks have drawn increased attention and have been incorporated into a variety of materials to give high charge carrier mobilities, enhanced solution and solid-state fluorescence, and materials with reduced and low band gaps.[6−9] One limitation of traditional *N*-alkyl- and *N*-arylDTP building blocks, however, is the high energy of the DTP HOMO, which limits stability and the effective application of DTP-based materials to various devices. As a solution to this limitation, a new class of DTPs incorporating N-acyl groups were introduced by Evenson and Rasmussen in 2010, which exhibit stabilized HOMO and LUMO energy levels.[8,9] An alternate approach to stabilize the HOMO energy levels of such nitrogen-bridged systems was also introduced by Heeney and co-workers in 2010,[16] which replaced the thiophene backbone with thiazole to generate the analogous pyrrolo[2,3-*d*:5,4-*d*′]bisthiazole (PBTz, Chart 2).[16−19]

It must be pointed out that all previous reports on PBTz have given this fused-ring unit the name pyrrolo[3,2-*d*:4,5-*d*′]bisthiazole,[16−19] which actually describes the inverted isomer referred to as iso-PBTz here (Chart 2). Such oversights can be easy to miss, particularly for those less familiar with the subtleties of fused-ring nomenclature, and even the current authors initially overlooked this inversion and also used the

Received: October 10, 2017

ACS Publications © XXXX American Chemical Society

DOI: 10.1021/acs.joc.7b02570
J. Org. Chem. XXXX, XXX, XXX−XXX

Chart 2. Pyrrolobisthiazole Building Blocks

incorrect nomenclature in previous conference presentations. In order to assist the field with such complexities, an educational guide to fused-ring nomenclature has been recently published.[20] Although the synthesis of iso-DTP analogues have been recently described,[21,22] iso-PBTz building blocks have not yet been reported.

Although the reported PBTz-based materials do successfully exhibit the desired stabilization,[16−19] the electronic and optical properties of the PBTz units themselves have not been significantly characterized. To date, the only such reported characterization includes the electrochemistry of the triisopropylsilyl (TIPS) protected 4-dodecylPBTz, as well as that of the dibromoPBTz derivatives.[18] As such, this makes it difficult to compare the two relative approaches for stabilization (*N*-acylDTP vs PBTz) or to accurately quantify the electronic effects of the substitution of thiophene by thiazole.

In order to better understand the contributing structure−function relationships, and to make these new PBTz building blocks more readily available, the current report provides new synthetic methods and full optical and electronic characterization of the resulting PBTz products. In the process, the known family of PBTz building blocks has been suitably expanded, including the first reported examples of *N*-arylPBTz units. Lastly, the optical, electronic, and structural properties of the PBTz units have been compared to the analogous *N*-alkyl- and *N*-acylDTPs in order to fully quantify the relative electronic effects of the various methods utilized to tune the parent DTP building block.

RESULTS AND DISCUSSION

Synthesis. The new synthetic methods for the generation of *N*-alkyl- and *N*-arylPBTz monomers from 2,4-thiazolidinedione is given in Scheme 1. In comparison, the previous synthetic methods of both Heeney and Marder began with the commercially available 2-bromothiazole (Scheme 2).[16−19]

Scheme 1. New Synthetic Routes to PBTz Monomers

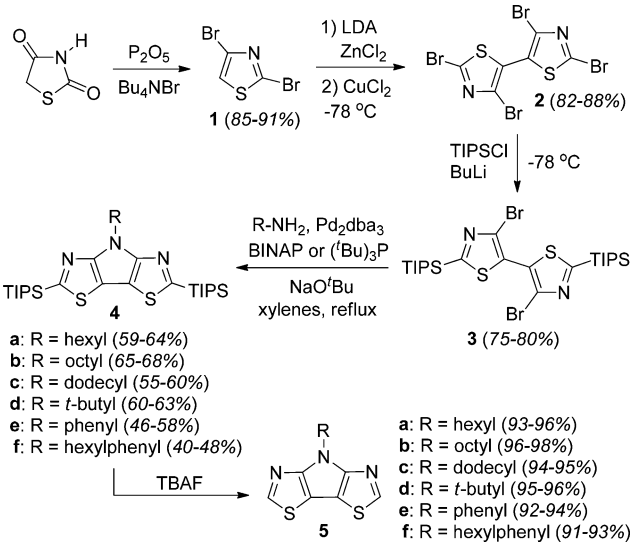

Scheme 2. Previous Synthetic Routes to TIPS-Protected PBTz Units

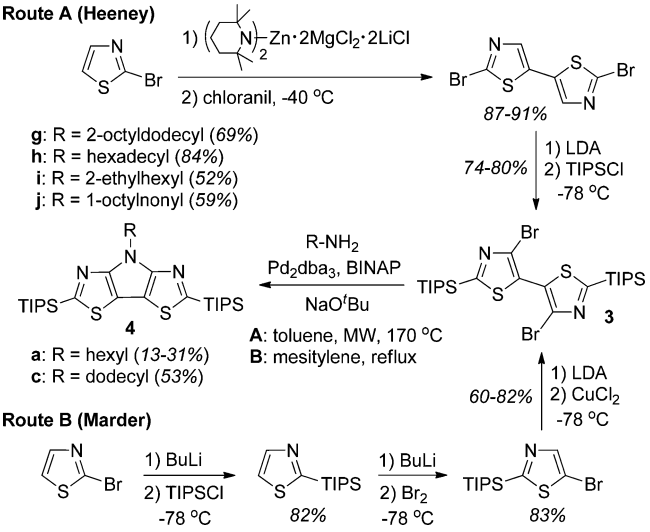

Marder and co-workers specifically point out that 2-bromothiazole is a preferable precursor over 2,4-dibromothiazole (**1**) due to the high cost of the latter.[23] While it is correct that commercial sources of **1** are nearly 10 times the cost of 2-bromothiazole, this cost can be reduced to less than half that of commercial 2-bromothiazole via the simple production of **1** from 2,4-thiazolidinedione as utilized here (Scheme 1).[24]

All three of the synthetic routes given in Schemes 1 and 2 converge at the synthesis of 4,4′-dibromo-2,2′-bis(triisopropylsilyl)-5,5′-bisthiazole (**3**) and differ primarily in the steps to generate this critical intermediate. The TIPS protecting group has been found to be critical, as Heeney and co-workers confirmed that the parent PBTz could not be generated directly from the unprotected 4,4′-dibromo-5,5′-bisthiazole.[16] Although they attributed this to competing Pd-catalyzed arylation reactions at the 2-positions of the thiazole ring, this is most likely due to the acidic nature of the 2-position of thiazole which would be readily deprotonated by the NaO^{t}Bu, thus potentially leading to various unwanted byproducts. Tangentially, the methods reported here also allowed the simple production of 4,4′-tetrabromo-2,2′-bis(trimethylsilyl)-5,5′-bisthiazole from **2**, but any attempts to produce trimethysilyl (TMS) protected PBTz units via this intermediate were unsuccessful. This was attributed to nucleophilic attack on the TMS silyl center by *t*-butoxide under the harsh reflux temperatures of xylene, leading to an anionic thiazole unit which can undergo additional chemistry or polymerization. It should be pointed out that, while the TIPS protecting groups enhance the stability of the PBTz unit, side reactions via oxidative coupling are still possible as evidenced by the isolation of the dimeric species 6,6′-bis(triisopropylsilyl)-2,2′-bis(4-hexylphenylpyrrolo[2,3-*d*:5,4-*d*′]bisthiazole) (**6**, see the Supporting Information).

The two previous routes to **3** both exploit the halogen dance[16,23,25] combined with an oxidative coupling step, with the methods largely differing in the order of which these two processes occur. In contrast, the methods reported here involved the generation of 2,2′,4,4′-tetrabromo-5,5′-bisthiazole

DOI: 10.1021/acs.joc.7b02570
J. Org. Chem. XXXX, XXX, XXX−XXX

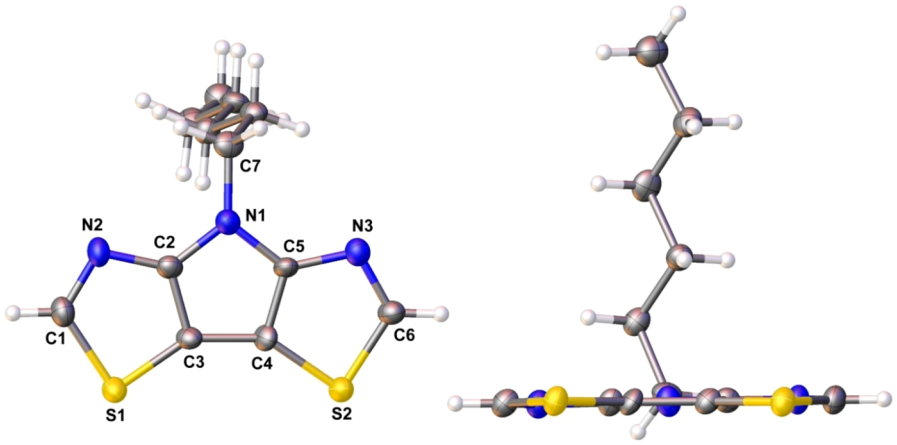

Figure 1. Face and edge ellipsoid plots of PBTz **5a** at the 50% probability level.

(**2**) via conditions developed by Evenson and Rasmussen for the production of 3,3′-dibromo-2,2′-bithiophene,[8] followed by exchange of the α-bromides for TIPS protecting groups. Compound **2** is the second tetrabromobisthiazole to be reported, following the analogous 4,4′-bisthiazole isomer reported in 2000.[26] These new methods allow the production of **3** from 2,4-thiazolidinedione with an overall yield of 52−64%. In comparison to the previous routes from 2-bromothiazole, this is an improvement over the methods of Marder and co-workers (overall yield of 41−55%), although it does fall short of the methods of Heeney and co-workers (overall yield of 64−73%). However, in addition to the reduction in cost, the new methods can be accomplished with common and readily available reagents.

All three routes use nearly identical methods for the conversion of **3** to the desired PBTz units via the TIPS-protected PBTz monomers **4** generated through Buchwald−Hartwig amination. The initial amination step is based on fairly standard conditions previously developed for the production of DTPs,[6] with the primary differences between the various routes being the solvent and corresponding temperatures applied. The methods of Heeney and co-workers utilize the most common solvent (toluene), but require a pressurized vial and microwave heating to achieve a temperature of 170 °C, with average yields of ca. 60%.[16] The methods of Marder and co-workers employed mesitylene at reflux to achieve temperatures of ca. 165 °C, but with much lower yields.[18] In comparison, the methods here utilize xylenes and modified conditions of those initially developed by Rasmussen and co-workers for the amination of 3-bromothiophene.[27] The modifications consist primarily of a more rigorous reflux, allowing temperatures of ca. 140 °C, and longer reaction times to give average yields of ca. 60%. As such, these conditions prove as effective as the previous methods of Heeney and co-workers, but do not require any specialized instrumentation. It should be pointed out that these conditions failed to successfully produce the *t*-butyl analogue **4d**, although **4d** could be successfully produced via the application of $(^t\mathrm{Bu})_3\mathrm{P}$ rather than BINAP as the ligand. This is consistent with previous limitations of BINAP in the production of various DTPs, including the *t*-butylDTP.[6] In all cases, the TIPS-protected PBTz monomers could be deprotected via tetrabutylammonium fluoride (TBAF) in near quantitative yields.

Crystallography. X-ray quality crystals of the TIPS-protected PBTz **4d** were grown by slow evaporation of a diethyl ether solution, while crystals of the deprotected parent PBTz **5a** were grown by melting solid **5a** on the walls of a vial and allowing the melt to crystallize. Thermal ellipsoid plots of **5a** are given in Figure 1, and selected bond lengths of **5a** and **4d** are given in Table 1, along with previously reported data for

Table 1. Experimental Bond Lengths of Pyrrolo[2,3-*d*:5,4-*d*′]bisthiazoles 5a, 4d, and 4a, Compared to Dithieno[3,2-*b*:2′,3′-*d*]pyrroles 7 and 8

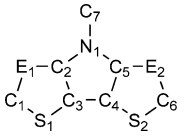

5 E = N
4a E = N
4d E = N
7 E = C
8 E = C

bond	5a	4d	4a[a]	7[b]	8[c]
S1−C1	1.761(8)	1.768(2)	1.768(2)	1.719(3)	1.720(2)
S1−C3	1.703(7)	1.703(3)	1.718(2)	1.716(3)	1.709(2)
C1−E1	1.31(1)	1.318(3)	1.325(3)	1.349(6)	1.341(3)
E1−C2	1.36(1)	1.363(3)	1.361(3)	1.416(5)	1.422(3)
C2−C3	1.39(1)	1.397(3)	1.387(3)	1.384(4)	1.369(3)
N1−C2	1.38(1)	1.394(3)	1.383(3)	1.379(5)	1.402(2)
C3−C4	1.43(1)	1.418(3)	1.413(3)	1.420(4)	1.431(2)
N1−C7	1.45(1)	1.495(3)	1.457(3)	1.451(4)	1.392(2)

[a]Reference 18. [b]Reference 7. [c]Reference 8.

the TIPS-protected PBTz **4a**,[18] *N*-octylDTP (**7**),[7] and *N*-octanoylDTP (**8**)[8] for comparison. As with previously reported structures of DTPs, the fused-ring PBTz **5a** is completely flat with no evidence of bowing.

The bond lengths and angles of all three PBTz species are in good agreement, although the PBTz structures exhibit some marked differences from DTPs **7** and **8**. Most notably are a considerable shortening of both N−C bonds of the thiazole ring in comparison to the analogous C−C bonds of the DTP thiophenes. This shortening of these two exterior bonds of the PBTz structure then results in a considerable elongation of the external S−C bond (i.e., S1−C1). These structural differences are consistent with the differences between the parent thiophene and thiazole heterocycles,[28] although the elongation of the PBTz S−C bond is significantly greater than that observed in the parent thiazole. In contrast, the central pyrrole ring of PBTz exhibits quite good agreement with that of DTP.

DOI: 10.1021/acs.joc.7b02570
J. Org. Chem. XXXX, XXX, XXX−XXX

The greatest effect of these structural differences is a vertical displacement of the α-carbons of the PBTz unit relative to the fused backbone. As a consequence, exterior bonds to these α-positions adopt a near-perfect coplanar orientation with the C3−C4 bond connecting the two thiazole rings of the PBTz (see Figure S25 in the Supporting Information). In contrast, the exterior bonds of DTP exhibit a downward cant of ca. 4° relative to the DTP backbone. As a result, PBTz-based conjugated materials should exhibit a more linear rodlike structure than the analogous DTPs. An example of this linear rodlike structure can be seen in the PBTz dimer **6** (Figure S24), and the enhanced linear nature of PBTz materials could lead to enhanced packing effects in the solid state. Lastly, the observed structural differences also result in the PBTz unit being slightly smaller than the corresponding DTP.

The packing of **5a** consists of one-dimensional ribbons via S···N short contacts,[29] as well as associated S···H−C contacts. These ribbons arrange in parallel arrangements separated by ca. 11.43 Å, the space between which are occupied by the hexyl side chains. Above and below each ribbon is another layer of parallel ribbons, with each layer roughly perpendicular to the next. The layers of perpendicular ribbons are again connected via S···N and S···H−C short contacts, with the same sulfur on each PBTz providing both linear and perpendicular contacts. The linear S···N contacts are 3.064 Å (less than the sum of the van der Waals radii at 3.35 Å[30]) with a C−S···N angle of 164°, while the perpendicular S···N contacts are slightly longer at 3.078 Å with a C−S···N angle of 176°. Such S···N contacts have also been observed for the 2,6-dibromo derivative of **5a**, although to a lesser degree (S···N contacts are 3.241 Å).[18] The sulfur of each S···N contact is simultaneously involved in a short contact to the hydrogen on the α-carbon adjacent to the nitrogen, in which the linear S···H−C contacts are 2.918 Å and the perpendicular S···H−C contacts are slightly shorter at 2.872 Å. However, as the S···H−C angles are 107° and 109°, respectively, these interactions are expected to be extremely weak and are most likely just an artifact of the more prominent S···N interaction. The presence of such S···N interactions, in addition to the typical S···S commonly seen in thiophene-based materials, could again contribute modified packing motifs for PBTz-based materials in comparison to DTP-based materials.

Electrochemistry. In order to quantify the extent of electronic stabilization resulting from the replacement of the thiophene rings of DTP with thiazole, the TIPS-protected PBTz series **4a−f** and the parent PBTz series **5a−f** were characterized by cyclic voltammetry. The electrochemical data of the PBTz series **5a−f** are given in Table 2, as well as the data for the *N*-alkyl- and *N*-acylDTPs **7** and **8** for comparison. The data for the TIPS-protected PBTz series **4a−f** are given in Table S2 in the Supporting Information.

All of the TIPS-protected PBTz species exhibit a quasireversible oxidation assigned as the oxidation of the conjugated backbone. The quasireversible nature here is due to the steric bulk of the TIPS groups[32] which prevents coupling of the radical cation generated by the oxidative process. The alkyl-functionalized series **4a−d** exhibit an $E_{1/2}$ of 0.78 V, which agrees well with the previously reported voltammogram of **4c**.[18] The 4-arylPBTz species **4e** and **4f**, however, exhibit a further stabilization of ca. 100 mV, which is consistent with the stabilization of *N*-arylDTPs in comparison to the *N*-alkyl analogues.[7] In comparison, the deprotected PBTz series **5a−f** exhibit a well-defined irreversible oxidation, again assigned to

Table 2. Electrochemical Data for PBTz and DTP Units[a]

compound	R	E_p (V)[a]	E_{onset} (V)	E_{HOMO} (eV)[b]
5a	C_6H_{13}	0.98	0.87	−6.0
5b	C_8H_{17}	0.98	0.87	−6.0
5c	$C_{12}H_{25}$	0.98	0.87	−6.0
5d	^{t}Bu	0.96	0.86	−6.0
5e	Ph	1.05	0.97	−6.1
5f	C_6H_{13}Ph	1.04	0.95	−6.1
7[c]	C_8H_{17}	0.51	0.45	−5.6
8[c]	COC_7H_{15}	0.73	0.67	−5.8

[a]All potentials vs Fc/Fc^+. [b]$E_{HOMO} = -(E_{[onset, ox vs Fc^+/Fc]} + 5.1)$ (eV), ref 31. [c]ref 8.

oxidation of the conjugated backbone. Without the steric protection of the TIPS groups, the radical cations generated undergo rapid coupling typical of thiophene species, thus accounting for the irreversible nature of the oxidation. As the TIPS groups are also electron donating,[32,33] their removal results in a positive shift of ca. 200 mV in the peak potentials (E_{pa}) of the deprotected PBTz series **5a−f** (Table 2). No reduction processes were observed within the electrochemical solvent window utilized, which is consistent with the predicted value of ca. −2.9 V for the PBTz reduction.

As the TIPS groups of **4a−f** alter the electronic nature of the PBTz core, the deprotected PBTz units provide the most accurate measure of the electronic stabilization in comparison to DTP. As shown in Table 2 and Figure 2, direct comparison

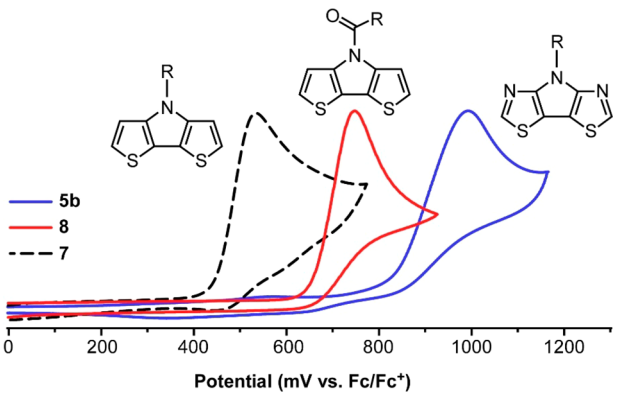

Figure 2. Comparative voltammograms of PBTz **5b**, *N*-octyl DTP **7**, and *N*-octanoyl DTP **8**.

of PBTz **5b** to DTPs **7** and **8** reveals that PBTz provides substantial stabilization even over the *N*-acylDTP **8**. In fact, the stabilization of the 4-alkylPBTz in comparison to the analogous *N*-alkylDTP is essentially twice that of the stabilization afforded by the *N*-acylDTP. Thus, a near linear trend is observed in the corresponding HOMO energies, with values of −5.6 eV for the *N*-alkylDTP, −5.8 eV for the *N*-acylDTP, and −6.0 eV for the 4-alkylPBTz. In addition, all of these values can be further stabilized by ca. 0.1 eV by using the corresponding aryl analogues, thus allowing continuous tuning of the HOMO energies over the range of −5.6 to −6.1 eV.

UV−vis Spectroscopy. The spectroscopic data for the PBTz series **5a−f** are given in Table 3, as well as the data for the *N*-alkyl- and *N*-acylDTPs **7** and **8** for comparison. Comparative UV−visible spectra of **5b**, **7**, and **8** are shown in Figure 3. All of the 4-alkylPBTz species exhibit a single transition centered at ca. 305 nm, although weakly defined

DOI: 10.1021/acs.joc.7b02570
J. Org. Chem. XXXX, XXX, XXX−XXX

Table 3. UV−Visible Absorption Data for PBTz and DTP Units[a]

compound	λ_{max} (nm)	ε (M^{-1} cm^{-1})	λ_{max} (nm)	ε (M^{-1} cm^{-1})
5a	306	15100		
5b	305	14700		
5c	304	14200		
5d	306	16600		
5e	300	18000	245	15700
5f	305	12700	246	10300
7[b]	310	26100	298	29300
8[c]	305	15400	289	27600

[a]In $CHCl_3$. [b]In CH_2Cl_2, ref 7. [c]In CH_3CN, ref 8.

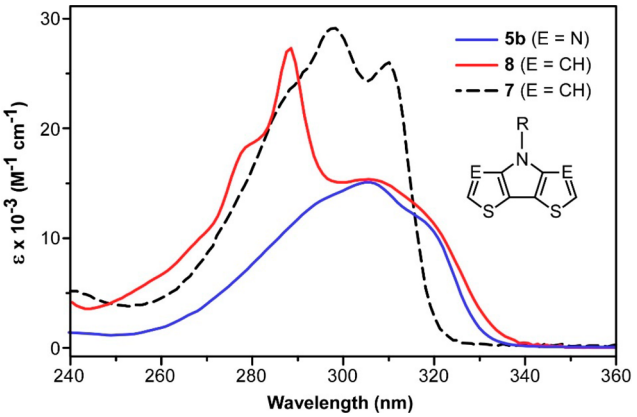

Figure 3. Comparative UV−visible spectra of PBTz **5b** (in $CHCl_3$), and DTPs **7** (in CH_2Cl_2), and **8** (in CH_3CN).

shoulders can be observed at both lower and higher energy. Due to the close energetic spacing of these transitions (ca. 1400 cm^{-1}), these shoulders are assigned as vibrational components of the same electronic transition. The 4-aryl analogues **5e** and **5f** exhibit similar transitions near 305 nm, although with a less defined structure. In addition, the aryl analogues exhibit a second higher-energy transition at ca. 245 nm, which is assumed to involve the π-system of the aryl substituent.

The overall structure of absorbance for the 4-alkylPBTz species is similar to that of *N*-alkylDTPs, although not as strongly defined and with onsets red-shifted by ca. 10 nm. As it has already been established above, that the HOMO energy levels of the PBTz units are significantly stabilized in comparison to DTP. Thus, this red shift indicates that the PBTz LUMO is similarly stabilized, but to a greater extent. In comparison to the *N*-acylDTPs, the 4-alkylPBTz absorbance onset is very slightly blue-shifted with a very similar shape to lower-energy transition of the *N*-acylDTP. This is notable as the *N*-acylDTP transition has been assigned to be of at least partial charge transfer (CT) character,[8] although there is currently no evidence of any CT character in the PBTz transition. Marder and co-workers reported the DFT-calculated molecular orbital surfaces for the PBTz HOMO and LUMO,[18] which were found to be nearly identical to that previously determined for DTP.

The most notable aspect of the PBTz absorbance, however, is the significant reduction in molar absorptivity (ε) compared to the DTPs. Typical values for *N*-alkylDTPs are 25 000−30 000 M^{-1} cm^{-1}, while the analogous 4-alkylPBTz values given in Table 3 are only 14 000−16 000 M^{-1} cm^{-1}. This trend in reduced absorptivity has been previously reported for other cases in which thiophene has been replaced by thiazole,[34−36] and computational studies have shown that the transition oscillator strength continues to decrease with each additional substitution by thiazole.[37] Even the parent heterocycles themselves exhibit this difference in absorptivity. Although the absorbance energies of thiophene and thiazole are very similar (231 vs 233 nm), the molar absorptivity of thiazole is only 3700 M^{-1} cm^{-1} in comparison to 7400 M^{-1} cm^{-1} for thiophene.[38]

No significant explanation for this difference in absorptivity has been previously reported, yet what is known is that molar absorptivity is related to both the allowedness of the transition and the cross-sectional area of the chromophore.[39] While it is likely that the transition allowedness is influenced by electronic differences between thiophene and thiazole, it is well established that the thiazole ring is smaller than thiophene,[40] which should lead to a reduction in the maximum possible cross-sectional area of thiazole analogues and lower absorptivity. As can been seen in the overlay of the DTP and PBTz crystal structures given in Figure S25, PBTz is smaller than DTP, but not by enough to account for the extent of the differences in the corresponding molar absorptivities. Nevertheless, this reduced absorptivity could limit the effectiveness of PBTz-based materials in applications for which the extent of light absorbance is critical, such as photovoltaics.

CONCLUSIONS

An alternate and practical synthetic route to pyrrolo[2,3-*d*:5,4-*d*′]bisthiazole (PBTz) building blocks has been presented, starting from the inexpensive 2,4-thiazolidinedione. In the process, the scope of the known PBTz family has been expanded with four new members, including the first reported 4-arylPBTz units. More critically, the significant characterization of the PBTz unit has been presented for the first time, including the first crystal structure of a deprotected parent PBTz unit. As such, it has allowed the direct comparison of the two relative approaches for stabilization of the more commonly applied dithieno[3,2-*b*:2′,3′-*d*]pyrrole (DTP) building blocks (i.e., *N*-acyl functionalization of DTP vs PBTz) and to accurately quantify the electronic effects of the substitution of thiophene by thiazole. This has revealed that the PBTz unit allows the greatest extent of stabilization of the HOMO energy level and, when combined with the currently known family of DTP building blocks, these HOMO levels can be finely tuned in increments of ca. 0.1 eV over the range of −5.6 eV for *N*-alkylDTPs to −6.1 eV for 4-arylPBTz units. However, although PBTz units provide the greatest extent of HOMO stability, the optical characterization of these species has also revealed that they exhibit the greatest reduction in molar absorptivity. As such, the limited absorbance efficiency of these building blocks could limit the effectiveness of PBTz-based materials in applications such as photovoltaics.

EXPERIMENTAL SECTION

General Information. 2,4-Dibromothiazole (**1**) was prepared as previously reported.[24] Xylenes and THF were distilled from sodium/benzophenone prior to use. $CHCl_3$ and CH_2Cl_2 were dried with $MgSO_4$ and filtered through a silica plug prior to use. $ZnCl_2$ and $CuCl_2$ were dried in vacuo, and all other materials were reagent-grade and used without further purification. All glassware was oven-dried, assembled hot, and cooled under a N_2 atmosphere. Chromatography was performed using standard methods, with 230−400 mesh silica gel

DOI: 10.1021/acs.joc.7b02570
J. Org. Chem. XXXX, XXX, XXX−XXX

in 1 in. diameter columns. Melting points were obtained with a digital thermocouple, accurate to 0.1 °C resolution. NMR spectroscopy was performed on a Bruker 400 MHz spectrometer in $CDCl_3$ solvent. All NMR spectra are referenced to the chloroform resonance at 7.26 ppm, and multiplicity is as follows: s = singlet, d = doublet, t = triplet, quin = quintet, sep = septet, m = mulitplet. HRMS (ESI-TOF) was performed in-house.

2,2′,4,4′-Tetrabromo-5,5′-bisthiazole (2). A 250 mL three-neck round-bottom flask was equipped with a 125 mL addition funnel, to which the solids 2,4-dibromothiazole (3.64 g, 15 mmol) and $ZnCl_2$ (2.45 g, 18 mmol) were added. The complete system was then evacuated and backfilled with N_2 three times. THF (75 mL) was added to the flask and cooled to 0 °C. Diisopropylamine (2.55 mL, 18.0 mmol) and butyllithium (7.2 mL, 2.5 M in hexanes, 18 mmol) were added, and the solution stirred for 30 min at 0 °C before cooling to −78 °C via an acetone/CO_2 bath. THF (75 mL) was then added to the addition funnel, and the funnel contents were added dropwise to the lithium diisopropylamide solution, which was then stirred for 1 h 45 min. The flask was warmed to room temperature over 15 min, and then cooled again to −78 °C. $CuCl_2$ was added (2.42 g, 18.0 mmol) and the solution was stirred for 30 min. Dry air was bubbled into the reaction for 2 min, and the flask was left in the cryogenic bath overnight, warming slowly to room temperature. The following day, saturated aqueous NH_4Cl was added and the mixture was extracted with $CHCl_3$. The organic fractions were combined and dried with $MgSO_4$, and the solvent was removed in vacuo to give a brown solid. The solid was then washed well with methanol to give 2.96−3.17 g of a light tan powder (82−88% yield). mp 224.1−225.6 °C. ^{13}C NMR: δ 138.0, 126.5, 125.4. HRMS (m/z): calcd for $C_6N_2S_2Br_4^{79}$ $[M + H]^+$ 480.6315, found 480.6291.

4,4′-Dibromo-2,2′-bis(triisopropylsilyl)-5,5′-bisthiazole (3). Bisthiazole **2** (1.45 g, 3.0 mmol) was added to a 500 mL three-neck round-bottom flask, which was then placed under a N_2 atmosphere. THF (250 mL) and triisopropylsilyl chloride (1.41 mL, 6.6 mmol) were then added, and the mixture cooled to −78 °C in an acetone/CO_2 bath. Butyllithium (2.64 mL, 2.5 M in hexanes, 6.6 mmol) was added, the solution was stirred at −78 °C for 2 h, and the reaction was allowed to warm to room temperature overnight. Saturated aqueous NH_4Cl was then added, and the mixture was extracted with $CHCl_3$. The combined organic layers were dried with $MgSO_4$ and concentrated to give a brown oily solid that was purified via column chromatography (20% $CHCl_3$ in hexanes) to yield 1.43−1.53 g of a yellow microcrystalline solid (75−80% yield). mp 109.7−110.9 °C (Lit.[16] 112−114 °C). ^1H NMR: δ 1.47 (sept, J = 7.4 Hz, 36H), 1.18 (d, J = 7.4 Hz, 6H). ^{13}C NMR: δ 172.5, 130.3, 125.0, 18.44, 11.56. All NMR values agree with previously reported values.[16,21]

General Synthesis of 4-Functionalized 2,6-Bis(triisopropylsilyl)-4*H*-pyrrolo[2,3-*d*:5,4-*d*′]bisthiazoles. Sodium *tert*-butoxide (0.461 g, 4.8 mmol), $Pd_2(dba)_3$ (0.046 g, 5 mol %), bisthiazole **3** (0.638 g, 1.0 mmol), and BINAP (0.125 g, 20 mol %) were added to a 50 mL round-bottom flask equipped with a reflux condenser. Xylenes (25 mL) were added, and the mixture stirred for 20 min. The appropriate amine was added (1.4 mmol), and the solution heated at vigorous reflux for 20 h. Water was then added and the mixture was extracted with diethyl ether. The combined organic layers were then dried with $MgSO_4$ and concentrated in vacuo, and the resulting solid was purified via column chromatography (hexanes) to give a dark yellow microcrystalline material.

*4-Hexyl-2,6-bis(triisopropylsilyl)-4H-pyrrolo[2,3-d:5,4-d′]-bisthiazole (**4a**).* 340−370 mg (59−64% yield); mp 74.9−76.0 °C. ^1H NMR: δ 4.62 (d, J = 6.7 Hz, 2H) 2.04 (quin, J = 6.7 Hz, 2H), 1.47 (sep, J = 7.5 Hz, 6H), 1.28 (m, 6H), 1.19 (d, J = 7.5 Hz, 36H), 0.90 (t, J = 6.7 Hz, 3H). ^{13}C NMR: δ 166.4, 158.5, 106.7, 45.3, 31.3, 29.7, 26.4, 22.5, 18.6, 14.0, 11.8. ^1H NMR values agree with previously reported values.[18]

*4-Octyl-2,6-bis(triisopropylsilyl)-4H-pyrrolo[2,3-d:5,4-d′]-bisthiazole (**4b**).* 393−412 mg (65−68% yield); mp 58.4−60.3 °C. ^1H NMR: δ 4.61 (t, J = 6.7 Hz, 2H), 2.05 (quin, J = 6.7 Hz, 2H) 1.46 (sep, J = 7.4 Hz, 6H), 1.31 (m, 4H), 1.21 (m, 6H) 1.18 (d, J = 7.4 Hz, 36H) 0.85 (t, J = 6.7 Hz, 3H). ^{13}C NMR: δ 166.4, 158.5, 106.7, 45.3, 31.8, 29.8, 29.1(3), 29.1(1), 26.8, 22.7, 18.6, 14.1, 11.8. HRMS (m/z): calcd for $C_{32}H_{60}N_3S_2Si_2$ $[M + H]^+$ 606.3762, found 606.3776.

*4-Dodecyl-2,6-bis(triisopropylsilyl)-4H-pyrrolo[2,3-d:5,4-d′]-bisthiazole (**4c**).* 364−406 mg (55−60% yield); mp 35.8−37.1 °C. ^1H NMR: δ 4.61 (t, J = 6.7 Hz, 2H), 2.04 (quin, J = 6.7 Hz, 2H) 1.48 (sep, 6H, J = 7.5 Hz), 1.28 (m, 18H), 1.19 (d, J = 7.5 Hz, 36H), 0.90 (t, J = 6.7 Hz, 3H). ^{13}C NMR: δ 166.4, 158.5, 106.7, 45.3, 31.9, 29.8, 29.6(8), 29.6(5), 29.6(4), 29.5, 29.4, 29.1, 26.7, 22.7, 18.6, 14.1, 11.8. All NMR values agree with previously reported values.[18]

*4-Phenyl-2,6-bis(triisopropylsilyl)-4H-pyrrolo[2,3-d:5,4-d′]-bisthiazole (**4e**).* 262−331 mg (46−58% yield); mp 87.7−89.2 °C. ^1H NMR: δ 8.55 (d, J = 8.7 Hz, 2H), 7.60 (t, J = 7.6 Hz, 2H), 7.34 (t, J = 7.6 Hz, 1H), 1.52 (sep, J = 7.4 Hz, 6H) 1.22 (d, J = 7.4 Hz, 36H). ^{13}C NMR: δ 167.2, 157.1, 138.7, 128.9, 124.6, 120.9, 109.7, 18.6, 11.8. HRMS (m/z): calcd for $C_{30}H_{48}N_3S_2Si_2$ $[M + H]^+$ 570.2823, found 570.2833.

*4-(4-Hexylphenyl)-2,6-bis(triisopropylsilyl)-4H-pyrrolo[2,3-d:5,4-d′]bisthiazole (**4f**).* 262−314 mg (40−48% yield); mp 36.3−36.8 °C. ^1H NMR: δ 8.57 (d, J = 8.7 Hz, 2H), 7.34 (d, J = 8.7 Hz, 2H), 2.67 (t, J = 7.7 Hz, 2H), 1.69 (quin, J = 7.7 Hz, 2H), 1.52 (sep, J = 7.7 Hz, 6H), 1.40 (m, 6H), 1.19 (d, J = 7.7 Hz, 36H), 0.90 (t, J = 7.7 Hz, 3H). ^{13}C NMR: δ 167.0, 157.1, 139.3, 136.4, 128.7, 120.7, 109.4, 35.6, 31.8, 31.5, 28.9, 22.6, 18.6, 14.1, 11.8. HRMS (m/z): calcd for $C_{36}H_{60}N_3S_2Si_2$ $[M + H]^+$ 654.3762, found 654.3792.

*4-tert-Butyl-2,6-bis(triisopropylsilyl)-4H-pyrrolo[2,3-d:5,4-d′]-bisthiazole (**4d**).* Compound **4b** was prepared as above substituting $[(^tBu)_3P]BF_4$ for BINAP to give 330−347 mg (60−63% yield); mp 82.4−84.1 °C. ^1H NMR: δ 2.01 (s, 9H), 1.45 (sep, J = 7.4 Hz, 6H), 1.18 (d, J = 7.4 Hz, 36H). $^{13}CNMR$: δ 164.8, 158.2, 107.5, 59.3, 30.5, 18.6, 11.7. HRMS (m/z): calcd for $C_{28}H_{52}N_3S_2Si_2$ $[M + H]^+$ 550.3057, found 550.3166.

General Deprotection Methods to Generate 4-Functionalized 4*H*-pyrrolo[2,3-*d*:5,4-*d*′]bisthiazoles (5a−f). The TIPS-protected PBTz (0.4 mmol) was added a 50 mL round-bottom flask, followed by 15 mL of dry THF. Tetrabutylammonium fluoride (1.6 mL, 1.0 M in THF, 1.6 mmol) was added, and the reaction was stirred at room temperature for 4 h. A saturated aqueous NaCl solution was added to the reaction mixture, which was then extracted with diethyl ether. The combined organic layers were then dried with $MgSO_4$ and concentrated in vacuo. The resulting solid was purified via column chromatography (5% diethyl ether in hexanes) to afford the deprotected PBTz as a dark yellow microcrystalline solid.

*4-Hexyl-4H-pyrrolo[2,3-d:5,4-d′]bisthiazole (**5a**).* 99−102 mg (93−96% yield). mp 82.5−83.6 °C. ^1H NMR: δ 8.59 (s, 2H), 4.57 (t, J = 7.3 Hz, 2H) 2.02 (quin, J = 7.3 Hz, 2H), 1.31 (m, 6H), 0.85 (t, J = 7.3 Hz, 3H). ^{13}C NMR: δ 154.7, 149.0, 103.9, 45.6, 31.3, 30.1, 26.5, 22.5, 14.0. ^1H NMR values agree with previously reported values.[18]

*4-Octyl-4H-pyrrolo[2,3-d:5,4-d′]bisthiazole (**5b**).* 113−114 mg (96−97% yield). mp 69.1−69.9 °C. ^1H NMR: δ 8.60 (s, 2H), 4.57 (t, J = 7.4 Hz, 2H), 2.02 (quin, J = 7.4 Hz, 2H) 1.35 (m, 4H) 1.25 (m, 6H), 0.85 (t, J = 7.4 Hz, 3H). ^{13}C NMR: δ 154.7, 149.0, 103.9, 45.6, 31.7, 30.1, 29.1(4), 29.1(2), 26.8, 22.6, 14.1. HRMS (m/z): calcd for $C_{14}H_{20}N_3S_2$ $[M + H]^+$ 294.1099, found 294.1089.

*4-Dodecyl-4H-pyrrolo[2,3-d:5,4-d′]bisthiazole (**5c**).* 131−133 mg (94−95% yield). mp 48.6−48.8 °C. ^1H NMR: δ 8.59 (s, 2H), 4.57 (t, J = 7.2 Hz, 2H) 2.02 (quin, J = 7.2 Hz, 2H), 1.34 (m, 5H), 1.22 (m, 13H), 0.88 (t, J = 7.2 Hz, 3H). ^{13}C NMR: δ 154.7, 149.0, 103.9, 45.6, 31.9, 30.1, 29.6 (two carbons), 29.5(3), 29.4(7), 29.3, 29.2, 26.8, 22.7, 14.1.

*4-tert-Butyl-4H-pyrrolo[2,3-d:5,4-d′]bisthiazole (**5d**).* 90−91 mg (95−96% yield). mp 168.4−169.9 °C (dec). ^1H NMR: δ 8.56 (s, 2H), 2.01 (s, 9H). ^{13}C NMR: δ 154.6, 147.6, 104.8, 59.7, 30.4. HRMS (m/z): calcd for $C_{10}H_{12}N_3S_2$ $[M + H]^+$ 238.0473, found 238.0464.

*4-Phenyl-4H-pyrrolo[2,3-d:5,4-d′]bisthiazole (**5e**).* 95−97 mg (92−94% yield). mp 129.1−131.6 °C. ^1H NMR: δ 8.69 (s, 2H), 8.21 (d, J = 7.9 Hz, 2H), 7.57 (t, J = 7.9 Hz, 2H), 7.35 (t, J = 7.5 Hz, 1H). ^{13}C NMR: δ 153.8, 149.6, 137.4, 129.4, 126.2, 122.3, 106.4.

DOI: 10.1021/acs.joc.7b02570
J. Org. Chem. XXXX, XXX, XXX−XXX

HRMS (m/z): calcd for $C_{12}H_8N_3S_2$ $[M + H]^+$ 258.1060, found 258.1064.

*4-(4-Hexylphenyl)-4H-pyrrolo[2,3-d:5,4-d′]bisthiazole (**5f**).* 124–127 mg (91–93% yield). mp 68.9–70.3 °C. ^{1}H NMR: δ 8.67 (s, 2H), 8.03 (d, J = 8.5 Hz, 2H), 7.37 (d, J = 8.5 Hz, 2H), 2.68 (t, J = 7.7 Hz, 2H) 1.65 (quin, J = 7.7 Hz, 2H), 1.31 (m, 6H), 0.89 (t, J = 7.7 Hz, 3H). ^{13}C NMR: δ 153.8, 149.5, 141.2, 134.9, 129.3, 122.4, 106.0, 35.6, 31.8, 28.9, 22.7, 18.1, 14.1. HRMS (m/z): calcd for $C_{18}H_{20}N_3S_2$ $[M + H]^+$ 342.1099, found 342.1082.

UV–Visible Spectroscopy. UV–visible spectra were measured on a dual beam scanning spectrophotometer using samples prepared as dilute $CHCl_3$ solutions in matched 1 cm quartz cuvettes.

Electrochemistry. All electrochemical methods were performed utilizing a three-electrode cell consisting of a platinum disc working electrode, a platinum wire auxiliary electrode, and a Ag/Ag^+ reference electrode (0.10 M $AgNO_3$ in CH_3CN). Supporting electrolyte consisted of 0.10 M tetrabutylammonium hexafluorophosphate ($TBAPF_6$) in dry CH_2Cl_2. Solutions were deoxygenated by sparging with argon prior to each scan and blanketed with argon during the measurements. All measurements were collected at a scan rate of 100 mV/s and final potentials all reported relative to an internal ferrocene standard (50 mV vs Ag/Ag^+). E_{HOMO} values were estimated from the onset of oxidation in relation to ferrocene, using the value of −5.1 eV vs vacuum for ferrocene.[31]

X-ray Crystallography. X-ray quality crystals of **4d** and **6** were grown by slow evaporation of diethyl ether solutions, while crystals of **5a** were grown from cooling of molten samples. The X-ray intensity data of the crystals were measured at 100 K on a CCD-based X-ray diffractometer system equipped with a Cu X-ray tube (λ = 1.54178 Å) operated at 2000 W of power. The detector was placed at a distance of 5.047 cm from the crystal. Frames were collected with a scan width of 0.3° in ω and exposure time of 10 s/frame and then integrated with the Bruker SAINT software package using an arrow-frame integration algorithm. The unit cell was determined and refined by least-squares upon the refinement of XYZ-centeroids of reflections above 20$\sigma(I)$. The structure was refined using the Bruker SHELXTL (Version 5.1) Software Package.

■ ASSOCIATED CONTENT

Supporting Information

The Supporting Information is available free of charge on the ACS Publications website at DOI: 10.1021/acs.joc.7b02570.

NMR spectra for **2**, **3**, **4a–f**, **5a–f** (PDF)

Crystallographic data for **4d**, **5a**, **6** (CIF)

■ AUTHOR INFORMATION

Corresponding Author

*E-mail: seth.rasmussen@ndsu.edu.

ORCID

Seth C. Rasmussen: 0000-0003-3456-2864

Notes

The authors declare no competing financial interest.

■ ACKNOWLEDGMENTS

The authors thank North Dakota State University for support of this research and NSF-CRIF (CHE-0946990) for the purchase of departmental XRD instrument. We also wish to thank Dr. Angel Ugrinov (NDSU) for assistance with the collection of the X-ray crystal data and Dr. Bill Pennington (Clemson University) for helpful discussions about sulfur-nitrogen interactions.

■ REFERENCES

(1) *Handbook of Conducting Polymers*, 3rd ed.; Skotheim, T. A., Reynolds, J. R., Eds.; CRC Press: Boca Raton, FL, 2007.

(2) Rasmussen, S. C.; Ogawa, K.; Rothstein, S. D. In *Handbook of Organic Electronics and Photonics*; Nalwa, H. S., Ed.; American Scientific Publishers: Stevenson Ranch, CA, 2008; Vol. *1*, Chapter 1.

(3) *Handbook of Thiophene-based Materials*; Perepichka, I. F., Perepichka, D. F., Eds.; John Wiley & Sons: Hoboken, NJ, 2009.

(4) Baumgartner, T. *J. Inorg. Organomet. Polym. Mater.* **2005**, *15*, 389–409.

(5) Rasmussen, S. C.; Evenson, S. J.; McCausland, C. B. *Chem. Commun.* **2015**, *51*, 4528–4543.

(6) Rasmussen, S. C.; Evenson, S. J. *Prog. Polym. Sci.* **2013**, *38*, 1773–1804.

(7) Ogawa, K.; Rasmussen, S. C. *J. Org. Chem.* **2003**, *68*, 2921–2928.

(8) Evenson, S. J.; Rasmussen, S. C. *Org. Lett.* **2010**, *12*, 4054–4057.

(9) Evenson, S. J.; Pappenfus, T. M.; Delgado, M. C. R.; Radke-Wohlers, K.; Navarrete, J. T. L.; Rasmussen, S. C. *Phys. Chem. Chem. Phys.* **2012**, *14*, 6101–6111.

(10) Amb, C. M.; Chen, S.; Graham, K. R.; Subbiah, J.; Small, C. E.; So, F.; Reynolds, J. R. *J. Am. Chem. Soc.* **2011**, *133*, 10062–10065.

(11) Fei, Z.; Kim, J. S.; Smith, J.; Domingo, E. B.; Anthopoulos, T. D.; Stingelin, N.; Watkins, S. E.; Kim, J.-S.; Heeney, M. *J. Mater. Chem.* **2011**, *21*, 16257–16263.

(12) Gendron, D.; Morin, P.-O.; Berrouard, P.; Allard, N.; Aich, B. R.; Garon, C. N.; Tao, Y.; Leclerc, M. *Macromolecules* **2011**, *44*, 7188–7193.

(13) Green, J. P.; Han, Y.; Kilmurray, R.; McLachlan, M. A.; Anthopoulos, T. D.; Heeney, M. *Angew. Chem., Int. Ed.* **2016**, *55*, 7148–7151.

(14) Kato, T.; Imoto, H.; Tanaka, S.; Ishidoshiro, M.; Naka, K. *Dalton Transactions* **2016**, *45*, 11338–11345.

(15) Green, J. P.; Cryer, S. J.; Marafie, J.; White, A. J. P.; Heeney, M. *Organometallics* **2017**, *36*, 2632–2636.

(16) Al-Hashimi, M.; Labram, J. G.; Watkins, S.; Motevalli, M.; Anthopoulos, T. D.; Heeney, M. *Org. Lett.* **2010**, *12*, 5478–5481.

(17) Xia, R.; Al-Hashimi, M.; Tsoi, W. C.; Heeney, M.; Bradley, D. D. C.; Nelson, J. *Sol. Energy Mater. Sol. Cells* **2012**, *96*, 112–116.

(18) Getmanenko, Y. A.; Singh, S.; Sandhu, B.; Wang, C.-Y.; Timofeeva, T.; Kippelen, B.; Marder, S. R. *J. Mater. Chem. C* **2014**, *2*, 124–131.

(19) Patra, D.; Lee, J.; Lee, J.; Sredojevic, D. N.; White, A. J. P.; Bazzi, H. S.; Brothers, E. N.; Heeney, M.; Fang, L.; Yoon, M.-H.; Al-Hashimi, M. *J. Mater. Chem. C* **2017**, *5*, 2247–2258.

(20) Rasmussen, S. C. *ChemTexts* **2016**, *2*, 16.

(21) Martin, R.; Larsen, C. H.; Cuenca, A.; Buchwald, S. L. *Org. Lett.* **2007**, *9*, 3379–3382.

(22) Förtsch, S.; Bäuerle, P. *Polym. Chem.* **2017**, *8*, 3586–3595.

(23) Getmanenko, Y. A.; Tongwa, P.; Timofeeva, T. V.; Marder, S. R. *Org. Lett.* **2010**, *12*, 2136–2139.

(24) Uzelac, E. J.; Rasmussen, S. C. *J. Org. Chem.* **2017**, *82*, 5947–5951.

(25) Schnürch, M.; Spina, M.; Khan, A. F.; Mihovilovic, M. D.; Stanetty, P. *Chem. Soc. Rev.* **2007**, *36*, 1046–1057.

(26) Nussbaumer, T.; Neidlein, R. *Heterocycles* **2000**, *52*, 349–364.

(27) Ogawa, K.; Radke, K. R.; Rothstein, S. D.; Rasmussen, S. C. *J. Org. Chem.* **2001**, *66*, 9067–9070.

(28) Katritzky, A. R.; Pozharskii, A. F. *Handbook of Heterocyclic Chemistry*, 2nd ed.; Pergamon: Amsterdam, 2000; pp 61, 101.

(29) Politzer, P.; Murray, J. S.; Janjić, G. V.; Zarić, S. D. *Crystals* **2014**, *4*, 12–31.

(30) Weast, R. C., Ed. *Handbook of Chemistry and Physics*, 68th ed.; CRC Press, Inc.: Boca Raton, FL, 1987; p D-188.

(31) Cardona, C. M.; Li, W.; Kaifer, A. E.; Stockdale, D.; Bazan, G. C. *Adv. Mater.* **2011**, *23*, 2367–2371.

(32) Rucker, C. *Chem. Rev.* **1995**, *95*, 1009–1064.

(33) Panek, J. S.; Prock, A.; Eriks, K.; Giering, W. P. *Organometallics* **1990**, *9*, 2175–2176.

(34) Josse, P.; Chavez, P.; Dindault, C.; Dalinot, C.; McAfee, S.; Dabos-Seignon, S.; Tondelier, D.; Welch, G.; Blanchard, P.; Leclerc, N.; Cabanetos, C. *Dyes Pigm.* **2017**, *137*, 576–583.

DOI: 10.1021/acs.joc.7b02570
J. Org. Chem. XXXX, XXX, XXX–XXX

(35) Bronstein, H.; Collado-Fregoso, E.; Hadipour, A.; Soon, Y. W.; Huang, Z.; Dimitrov, S. D.; Ashraf, R. S.; Rand, B. P.; Watkins, S. E.; Tuladhar, P. S.; Meager, I.; Durrant, J. R.; McCulloch, I. *Adv. Funct. Mater.* **2013**, *23*, 5647−5654.
(36) Uzelac, E. J.; Rasmussen, S. C. *Eur. J. Inorg. Chem.* **2017**, *2017*, 3878−3883.
(37) Soto-Rojo, R.; Baldenebro-López, J.; Glossman-Mitnik, D. *Int. J. Photoenergy* **2016**, *2016*, 6479649.
(38) Katritzky, A. R.; Pozharskii, A. F. *Handbook of Heterocyclic Chemistry*, 2nd ed.; Pergamon: New York, 2000; pp 68, 115.
(39) Braude, E. A. *J. Chem. Soc.* **1950**, 379−384.
(40) Katritzky, A. R.; Pozharskii, A. F. *Handbook of Heterocyclic Chemistry*, 2nd ed.; Pergamon: New York, 2000; p 101.

DOI: 10.1021/acs.joc.7b02570
J. Org. Chem. XXXX, XXX, XXX−XXX